

Individual Differences in Delay Discounting are Associated with Dorsal Prefrontal Cortex Connectivity in Youth

Kahini Mehta^{1,2}, Adam Pines^{1,2}, Azeez Adebimpe^{1,2}, Bart Larsen^{1,2}, Dani S. Bassett^{3,4,8,9,10}, Monica E. Calkins², Erica Baller^{1,2}, Martin Gell^{1,11,12}, Lauren M. Patrick⁶, Raquel E. Gur^{2,7,8}, Ruben C. Gur^{2,7,8}, David R. Roalf², Daniel Romer⁵, Daniel H. Wolf², Joseph W. Kable⁶, Theodore D. Satterthwaite^{1,2,7}

1. Lifespan Informatics and Neuroimaging Center (PennLINC), Perelman School of Medicine, University of Pennsylvania, Philadelphia, PA 19104, USA
2. Department of Psychiatry, University of Pennsylvania, Philadelphia, PA, 19104, USA
3. Department of Bioengineering, School of Engineering and Applied Science, University of Pennsylvania, PA 19104, USA
4. Department of Electrical & Systems Engineering, University of Pennsylvania, PA 19104, USA
5. Annenberg Public Policy Center, University of Pennsylvania, Philadelphia, PA 19104, USA
6. Department of Psychology, University of Pennsylvania, Philadelphia, PA 19104, USA
7. Penn/CHOP Lifespan Brain Institute, University of Pennsylvania, Philadelphia, PA 19104, USA
8. Department of Neurology, University of Pennsylvania, Philadelphia, PA, 19104, USA
9. Department of Physics & Astronomy, University of Pennsylvania, Philadelphia, PA, 19104, USA
10. Santa Fe Institute, Santa Fe, NM, 87051, USA
11. Department of Psychiatry, Psychotherapy and Psychosomatics, Medical Faculty, RWTH Aachen University, Aachen, Germany
12. Institute of Neuroscience and Medicine (INM-7: Brain & Behaviour), Research Centre Jülich, Jülich, Germany

Corresponding author:

Theodore D. Satterthwaite, M.D.,
Associate Professor of Psychiatry,
Director, Penn Lifespan Informatics and Neuroimaging Center (PennLINC),
Perelman School of Medicine,
University of Pennsylvania,
www.pennlinc.io

Email address:

sattertt@pennmedicine.upenn.edu

Mailing address:

Richards Medical Labs, 5th floor
3700 Hamilton Walk,
Philadelphia, PA 19104

ABSTRACT

Delay discounting is a measure of impulsive choice relevant in adolescence as it predicts many real-life outcomes, including substance use disorders, obesity, and academic achievement. However, the functional networks underlying individual differences in delay discounting during youth remain incompletely described. Here we investigate the association between multivariate patterns of functional connectivity and individual differences in impulsive choice in a large sample of youth. A total of 293 youth (9-23 years) completed a delay discounting task and underwent resting-state fMRI at 3T. A connectome-wide analysis using multivariate distance-based matrix regression was used to examine whole-brain relationships between delay discounting and functional connectivity was then performed. These analyses revealed that individual differences in delay discounting were associated with patterns of connectivity emanating from the left dorsal prefrontal cortex, a hub of the default mode network. Delay discounting was associated with greater functional connectivity between the dorsal prefrontal cortex and other parts of the default mode network, and reduced connectivity with regions in the dorsal and ventral attention networks. These results suggest that delay discounting in youth is associated with individual differences in relationships both within the default mode network and between the default mode and networks involved in attentional and cognitive control.

KEYWORDS: delay discounting, youth, fMRI, functional connectivity, DMN, VAN

INTRODUCTION

Delay discounting (DD) is a measure of impulsive decision-making (Madden et al., 2003) that refers to preference for a smaller reward sooner rather than a larger reward later (Bickel et al., 2012; Epstein et al., 2010). DD predicts many real-life outcomes, such as academic achievement and social functioning (Hirsh et al., 2008; Mahalingam et al., 2016). Additionally, DD is considered an important transdiagnostic behavior that is altered across multiple clinical disorders that are characterized by impulsive decisions, including substance misuse, schizophrenia, and attention-deficit hyperactivity disorder (ADHD; Amlung et al., 2019; Chase et al., 2011; Weller et al., 2014; Ortiz et al., 2015; Lempert et al., 2019). A better understanding of the mechanisms of DD could thus inform decisions regarding early interventions for certain disorders, particularly in at-risk adolescents. However, studies that link functional brain networks defined using functional connectivity (FC) to DD in youth remain sparse. Here, we sought to understand how DD is related to individual differences in functional brain networks in a large sample of youth.

Many studies have used task-based fMRI to uncover the brain regions engaged during DD, especially key regions involved in reward valuation such as the ventral striatum and hubs of the default mode network (DMN) such as the ventromedial prefrontal cortex (vmPFC) and posterior cingulate cortex (PCC; Schüller et al., 2019; Souther et al., 2022; Kable and Glimcher, 2007; Peters and Büchel, 2010). A related but distinct approach links DD to FC at rest instead of task-based responses. Work using FC is motivated in part by behavioral data that has suggested DD is a stable trait that varies among individuals and is heritable (Kirby, 2009). FC has previously proven predictive of individual personality traits and has also been used successfully to identify neural correlates of DD (Kable and Levy, 2015). Studies of individual differences in FC related to DD often use a network-based framework, which is supported by prior research suggesting that DD relies upon interactions among multiple brain networks (Chen et al., 2017). Specifically, prior work in adults has linked impulsive choice during DD to individual differences in connectivity in regions involved in reward and valuation such as the striatum, vmPFC and PCC (Kable and Levy, 2015; Li et al., 2013; Calluso et al., 2015). Work in adults has also found that connectivity between the DMN and cognitive control networks such as the ventral attention and cingulo-opercular networks is predictive of delay discounting – increased functional connectivity between the two typically anticorrelated networks could disrupt cognitive control and impact decisions on DD tasks (Chen, Guo, Suo, and Feng, 2018). This is consistent with the idea of a role for top-down attentional/cognitive control in delay of gratification, as indicated in previous work (Hare et al., 2014; Mischel et al., 1989).

While there have been fewer studies of children and adolescents, prior work investigating ADHD has also related individual differences in DD to connectivity in regions important for valuation, such as the nucleus accumbens (Costa Dias et al., 2013). Similarly, work in both typically developing populations and children with ADHD indicates that cognitive control regions such as the dorsolateral prefrontal cortex (dlPFC) are related to DD in adolescents (Wang et al., 2017; Rosch et al., 2018). However, results from prior work in adolescents are for the most part heterogeneous, which may be driven by two factors. First, many studies of DD and functional networks in pediatric samples have been small, increasing the risk of type I error and reducing the likelihood of replicable results (Marek et al., 2022; Button et al., 2013). Second, many studies have

related DD to FC among a specific set of regions or limited set of networks, rather than evaluating the complete functional connectome. As DD is a complex cognitive process that engages multiple brain networks, such studies may not capture important differences in connectivity that are distributed across the cortex (Chen et al., 2017).

Accordingly, here we investigated how individual differences in DD are associated with connectome-wide differences in patterns of FC during adolescence. We capitalized on a large sample of 293 youth imaged as part of the Philadelphia Neurodevelopmental Cohort (Satterthwaite et al., 2014; Satterthwaite et al., 2016) who completed a DD task and resting-state fMRI. We conducted a connectome-wide association study (CWAS) to reveal DD-associated differences in the multivariate pattern of connectivity at each location in the brain (Shehzad et al., 2014; Sharma et al., 2017). While CWAS is a data-driven approach, we sought to test the hypothesis that individual differences in DD would be linked to connectivity in regions of both the DMN and networks involved in attentional control.

METHODS

Participants

This study considers participants who completed both neuroimaging and a DD task as part of the Philadelphia Neurodevelopmental Cohort (PNC; Satterthwaite et al., 2014); this sample largely overlaps with a previous report linking DD to individual differences in brain structure (Pehlivanova et al., 2018). Of the 1601 youths who completed neuroimaging as part of the PNC, 453 participants completed a behavioral DD task outside of neuroimaging sessions and were thus eligible for further analyses. Of these, $n=2$ did not meet the quality control criteria for behavioral data (Pehlivanova et al., 2018; see *DD task* section). Further, 21 participants were excluded for the following reasons: health conditions that could impact brain structure ($n=19$), scanning performed 12 months from the time of DD testing ($n=1$), and missing imaging data ($n=1$). An additional 137 participants were excluded due to poor quality scans, as described in the *Image quality assurance* section. Thus, a total of 293 participants (ages 9-23 years; $M=17.18$ years, $SD=3.10$ years; 156 females, 137 males) formed the sample for our analyses after quality control.

Ethics

This study received approval from the institutional review boards at the University of Pennsylvania and Children's Hospital of Philadelphia. All adult participants provided informed consent. For minors, parent or guardians provided informed consent and the minor provided assent.

DD task

The DD task consisted of 34 self-paced questions where the participant chose between a smaller amount of money available immediately or a larger amount available after a delay (Senecal et al., 2012; Pehlivanova et al., 2018). The smaller, immediate rewards ranged from \$10 to \$34, and the larger, delayed rewards were fixed at \$25, \$30, or \$35 with equal frequency. Delays ranged from 1 to 171 days. Trials and task procedures were identical in content and order for all participants. The DD task was administered as part of an hour-long web-based battery of neurocognitive tests

as part of a procedure used previously, on a separate day from the imaging session (Gur et al., 2010; Gur et al., 2012).

Discount rates from the DD task were calculated with hyperbolic discounting model of the form:

$$V=A/(1+kD),$$

where V is the subjective value of the delayed reward, A is the amount of the delayed reward, D is the delay in days, and k is the subject-specific discount rate (Mazur, 1987; Kable and Glimcher, 2010). As in previous work, the *fmincon* optimization algorithm in MATLAB (MathWorks) was used to estimate the best fitting k from each participant's choice data, assuming that choices were a logistic function of V s (Senecal et al., 2012; Pehlivanova et al., 2018). A higher k value indicates steeper discounting of delayed rewards and thus more impulsive choices. As the distribution of estimated k parameters is right-skewed, we applied a log-transform ($\log(k)$) before further analysis.

Quality assurance of DD data was conducted as described previously: each participant's responses were fit using a logistic regression model, with predictors including the immediate amount, delayed amount, delay, their respective squared terms, and two-way interaction terms (Pehlivanova et al., 2018). The goodness of fit of this model was assessed using the coefficient of discrimination (Tjur et al., 2009); a value less than 0.20 indicated nearly random choices and resulted in exclusion (Pehlivanova et al., 2018). As prior (Pehlivanova et al., 2018), we evaluated associations between $\log(k)$ and demographic variables using a linear model.

Image acquisition

All MRI scans were acquired using the same 3T Siemens (Erlangen, Germany) Tim Trio whole-body scanner and 32-channel head coil at the Hospital of the University of Pennsylvania. Image acquisition protocols are described in detail in previous work (Satterthwaite et al., 2014). Briefly, the magnetization-prepared, rapid acquisition gradient-echo T1-weighted (MPRAGE) image was acquired with the following parameters: TR = 1810 ms; TE = 3.5 ms; TI = 1100 ms, FOV = $180 \times 240 \text{ mm}^2$, matrix = 192×256 , effective voxel resolution = $0.938 \times 0.938 \times 1 \text{ mm}^3$. Resting-state fMRI scans were acquired with a single-shot, interleaved multi-slice, gradient-echo, echo planar imaging (GE-EPI) sequence sensitive to BOLD contrast with the following parameters: TR = 3000 ms; TE = 32 ms; flip angle = 90° ; FOV = $192 \times 192 \text{ mm}^2$; matrix = 64×64 ; 46 slices; slice thickness/gap = $3/0 \text{ mm}$, effective voxel resolution = $3.0 \times 3.0 \times 3.0 \text{ mm}^3$. Resting-state scans consisted of 124 volumes. In addition, a B0 field map was derived for application of distortion correction procedures, using a double-echo, gradient-recalled echo (GRE) sequence: TR = 1000 ms; TE₁ = 2.69 ms; TE₂ = 5.27 ms; 44 slices; slice thickness/gap = $4/0 \text{ mm}$; FOV = 240 mm; effective voxel resolution = $3.75 \times 3.75 \times 4 \text{ mm}^3$.

Image processing

Before the processing of both structural and functional data, a custom adolescent template was created with Advanced Normalization Tools (ANTs; Avants and Gee, 2004; Avants et al., 2011a). The template was created to minimize registration bias and maximize sensitivity to detect regional effects that can be impacted by registration error (Avants et al., 2011a). Structural images were then processed and registered to this template using the ANTs cortical thickness pipeline (Tustison et al., 2014). This procedure includes brain extraction, N4 bias field correction (Tustison et al., 2010), Atropos probabilistic tissue segmentation (Avants et al., 2011b), and the SyN diffeomorphic registration method (Avants et al., 2008; Klein et al., 2009).

The fMRI data were processed with an empirically validated preprocessing pipeline implemented in the eXtensible Connectivity Pipeline (XCP) Engine (Ciric et al., 2018). Resting-state time series preprocessing included correction of distortion induced by magnetic field inhomogeneity using FMRIB Software Library (FSL)'s FUGUE utility (Jenkinson, 2003), realignment of all volumes to a selected reference volume using MCFLIRT (Jenkinson et al., 2002), interpolation of intensity outliers in each voxel's time series using AFNI's 3dDespike utility and demeaning and removal of first- and second-order trends. After the despiking and detrending, the functional data were denoised using a 36-parameter confound regression model that has been shown to minimize associations with motion artifact and other nuisance variables (Ciric et al., 2017). Specifically, the confound regression model included the six framewise estimates of motion, the mean signal extracted from eroded white matter and cerebrospinal fluid compartments, the global signal, the derivatives of each of these nine parameters, and quadratic terms of each of the nine parameters as well as their derivatives. To avoid frequency mismatch, both the BOLD-weighted time series and the confound regressor timeseries were temporally filtered simultaneously using a first-order Butterworth filter with a passband between 0.01 and 0.08 Hz (Hallquist et al., 2013). Confound regression was performed using AFNI's 3dTproject. Denoised functional images were co-registered to the T1 image using boundary-based registration (Greve and Fischl, 2009) and aligned to the study-specific adolescent template using the ANTs transform for the T1 image as above. Functional images were resampled to 4 mm³ isotropic voxels in the template space before CWAS for computational feasibility (Shehzad et al., 2014). However, higher spatial resolution images (2 mm³) were used for follow-up seed-based analyses. Throughout, all transformations were concatenated so that only one interpolation was performed.

Image quality assurance

Some participants were excluded due to inadequate structural image quality (n=3), as determined by three expert raters (Rosen et al., 2017). As described in prior work (Satterthwaite et al., 2013; Ciric et al., 2018), a participant's resting-state fMRI data was excluded if the mean relative root mean square (RMS) framewise displacement was higher than 0.2 mm, or if it had more than 20 frames with motion exceeding 0.25 mm (n=133). One participant was also excluded when manual inspection revealed fewer data points than expected in the resting-state scan (n=1). Our final sample thus included 293 participants. Additionally, to account for residual motion in the data that passed quality assurance, we included RMS framewise displacement as a covariate in all models.

Multivariate distance-based matrix regression (MDMR)

We performed a CWAS using MDMR as described in detail in previous studies (Shehzad et al., 2014; Satterthwaite et al., 2015; Sharma et al., 2017). A schematic of the CWAS procedure is depicted in **Figure 1**. First, the preprocessed participant BOLD time series were used to conduct seed-based connectivity analyses at each voxel within gray matter. Specifically, Pearson's correlation coefficient between each voxel's time series and the time series of every other gray matter voxel (**Figure 1A & B**) was used to generate subject-level connectivity maps. Second, we summarized individual differences in FC maps by computing a distance matrix (also using Pearson's correlation) between the connectivity matrices for every possible pairing of participants (**Figure 1C**). Third, MDMR (**Figure 1D**) was used to test how well our phenotypic variable, $\log(k)$, explained variation in the distances between connectivity matrices across participants. This approach provided a measure of how FC patterns across participants were impacted by individual differences in $\log(k)$, while controlling for the effects of age, sex (assigned at birth), and in-scanner motion (Shehzad et al., 2014; Satterthwaite et al., 2015). MDMR yields a pseudo-F statistic for each voxel, whose significance was assessed using 5,000 iterations of a permutation test to generate a null distribution. The ultimate product of this procedure was a voxel-wise Z-statistic map describing the association between $\log(k)$ and the global pattern of connectivity for each voxel (**Figure 1E**). Aligning with current recommendations to minimize false positives, the type I error rate across voxels was controlled using cluster correction with a voxel height of $z > 3.09$ and utilized a cluster-extent probability threshold $p < 0.05$ (Eklund et al., 2016). We also ran an analysis to explore interactions with age and sex ($\log(k)*\text{age}$ or $\log(k)*\text{sex}$); these models included the same covariates listed above.

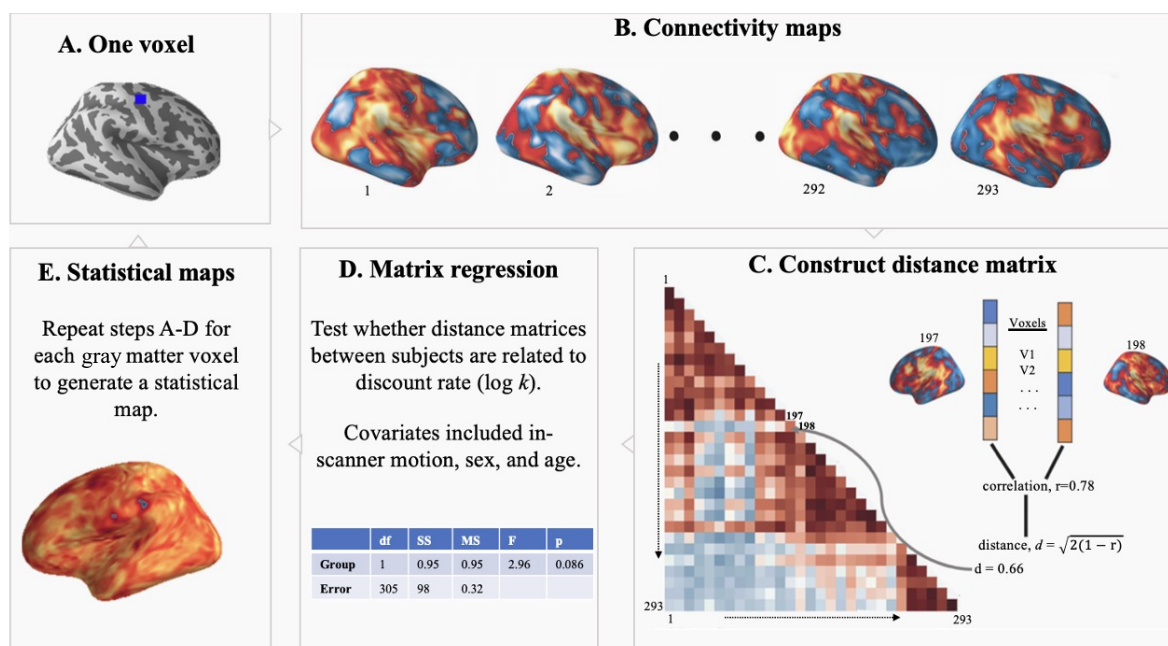


Figure 1. Connectome-wide analysis approach. For each gray matter voxel (A), a connectivity map was created for each subject (B), and the maps were compared in a pairwise manner (using correlation) to create a distance matrix (C). Multivariate distance-based matrix regression (MDMR) was used to evaluate how the multivariate patterns of

connectivity encoded by these distance matrices were associated with individual differences in delay discounting while controlling for age, sex, and in-scanner motion (**D**). Permutation testing yielded a pseudo- F statistic and a corresponding p value. This procedure was repeated for each gray matter voxel, yielding a voxel-wise statistical map (**E**).

Seed-based analyses

MDMR identified clusters where the overall multivariate pattern of connectivity is dimensionally related to DD, but it did not describe the specific pairwise FC patterns that drove the multivariate results. To characterize the direction of the effects, as in previous studies (Satterthwaite et al., 2015; Sharma et al., 2017), we conducted post-hoc seed-based descriptive analyses for each cluster returned by MDMR. Group-level seed analysis included age, sex, and in-scanner motion as covariates and was computed using a general linear model (implemented in FSL's *flameo*; Woolrich et al., 2004). These follow-up analyses were descriptive, as the seeds were selected based on the significance of the MDMR result.

Network enrichment testing

Given that neural activity differs across functional networks (Raut et al., 2020), we attempted to localize effects of interest within specific brain networks. Specifically, we examined whether associations with $\log(k)$ revealed by the seed-based analyses described above were located within one of the seven canonical large-scale brain networks (Yeo et al., 2011) using a conservative network enrichment testing procedure (see Baller et al., 2022 for details). To account for the different size of each network and the spatial autocorrelation of brain maps, statistical testing used a conservative spin-based spatial permutation procedure (Alexander-Bloch et al., 2018). Areas with positive and negative associations were evaluated separately. Briefly, statistical maps from the seed-based analysis were thresholded at $|z| \geq 3.09$ and projected onto a spherical representation of the cortical surface. This sphere was rotated 1,000 times per hemisphere to create a null distribution. For both the real and permuted data, we evaluated proportion of vertices that overlapped with each of the seven canonical functional networks. Networks were considered to have significant enrichment if the test statistic in the observed data was in the top 5% of the null distribution derived from permuted data.

Sensitivity analyses of socioeconomic status

To probe whether our results could be driven by individual differences in socioeconomic status (SES), mean parental education was included as a model covariate in addition to age, sex, and head motion.

RESULTS

Connectome-wide analyses identify a region of connectivity related to DD

We sought to determine whether and how individual differences in DD were associated with complex, multivariate patterns of FC in a large sample of youth. Notably, we found no significant correlation between $\log(k)$ and either age or sex. However, as these variables may be strongly associated with functional connectivity, they were included as model covariates in the connectome-wide analysis.

Our connectome-wide analysis using MDMR revealed that DD was related to a multivariate pattern of FC in the left dorsal prefrontal cortex (dPFC; cluster center of gravity: $x=30.9, y=43.8, z=30.3; k=12$ voxels, $p=1.03 \times 10^{-4}$; **Figure 2**). This finding suggested a pivotal role of the dPFC, a hub of the DMN (Alves et al., 2019; Andrews-Hanna et al., 2010), in DD-related activity. We additionally evaluated models that included interactions between DD and both sex and age; the interaction effects in these models were not statistically significant.

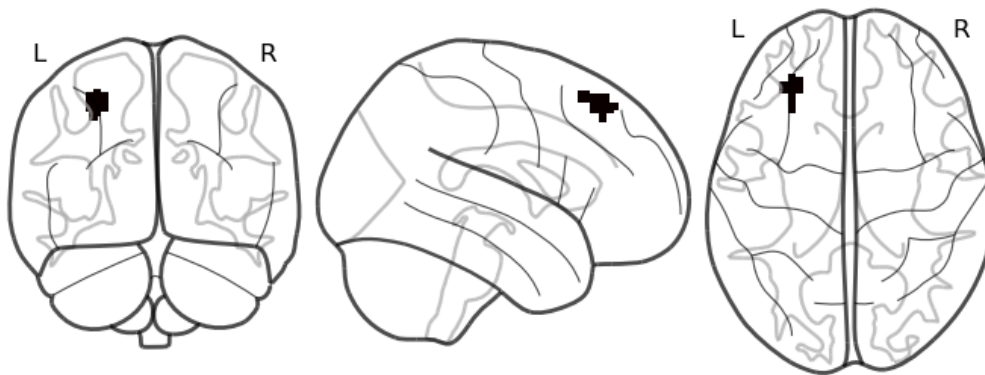


Figure 2. Connectome-wide analyses reveal that multivariate patterns of connectivity in the dorsal prefrontal cortex is associated with delay discounting. Volumetric depiction of the dorsal prefrontal cortex cluster identified by multivariate distance-based matrix regression. This dorsal prefrontal cortex cluster survived correction for multiple comparisons at $z>3.09, p<0.05$.

DD is related to individual differences in connectivity between attentional control and default mode networks

Having localized multivariate connectivity patterns associated with DD to the dPFC, we next sought to understand the individual differences in FC associated with DD that drove the observed MDMR results. We conducted seed-based connectivity analysis using the dPFC cluster identified by MDMR. In this general linear model, we included age, sex, and in-scanner motion as covariates.

We first evaluated the mean pattern of connectivity for the dPFC cluster. Across the entire sample, the left dPFC seed was strongly connected to elements of the DMN, including the PCC and vmPFC. The seed was anticorrelated mainly to regions within the dorsal attention network (DAN), such as the inferior parietal lobule, and regions in the ventral attention network (VAN) such as the temporoparietal junction (**Figure 3**). This connectivity profile suggests that the dPFC cluster was primarily affiliated with the DMN.

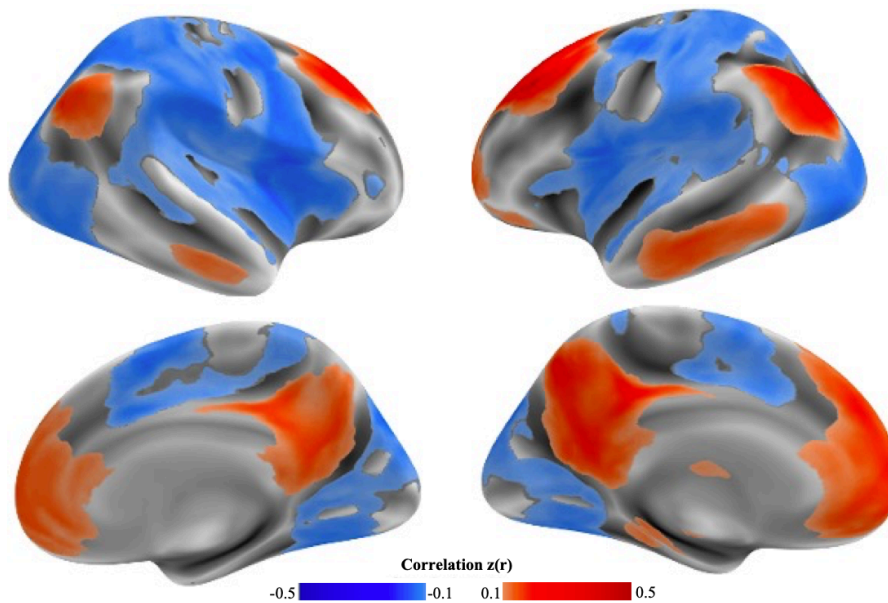


Figure 3. Mean connectivity of the dorsal prefrontal cortex cluster. The cluster identified by the connectome-wide association study (see Figure 2) was used as a seed to understand the connectivity profiles of the regions related to delay discounting. The left dorsal prefrontal cortex cluster had robust connectivity to other elements of the default mode network and was anticorrelated primarily with the dorsal and ventral attention network regions.

Next, we sought to determine how DD was associated with individual differences in FC from the dPFC seed identified by the connectome-wide analysis. Analysis of the cluster within the left dPFC revealed that higher rates of DD were correlated with increased connectivity between the dPFC and other elements of the DMN, including the PCC and lateral temporal cortex (**Figure 4**). In contrast, higher levels of DD were correlated with lower connectivity between the dPFC and regions within the VAN (including the temporoparietal junction and parts of the ventral frontal cortex) and the DAN (including the inferior parietal lobule and angular gyrus).

We next used spin-based network enrichment testing to statistically evaluate the spatial distribution of these effects. Enrichment testing revealed an enrichment of positive associations with $\log(k)$ in the DMN ($p=0.01$). In contrast, there was enrichment of negative associations in the DAN ($p=0.02$) and VAN ($p=1.5 \times 10^{-3}$). Together, these results could suggest that DD in youth is associated with individual differences connectivity within the DMN and between the DMN and attention networks. Specifically, higher rates of discounting (more impulsive choices) are associated with greater connectivity between the dPFC and other DMN regions, but lower connectivity between the dPFC and attentional control regions.

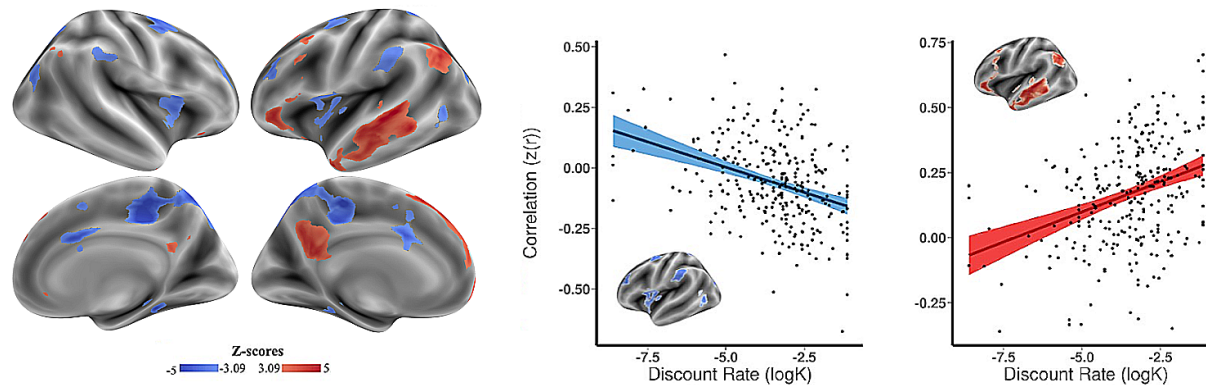


Figure 4. Individual differences in delay discounting are associated with dorsal prefrontal cortex connectivity to the default mode network, as well as control and attention networks. Follow-up seed-based analyses from the dorsal prefrontal cortex revealed that increased discount rate was associated primarily with increased connectivity with other elements of the default mode network (red), as well as diminished connectivity with mainly the dorsal and ventral attention network regions (blue). Maps represent patterns that drove the connectome-wide association study result rather than independent statistical tests. The maps are thresholded for display at $|z| > 3.09$, $p < 0.05$.

Sensitivity analyses

The dPFC cluster remained significant when SES was added as a model covariate as part of sensitivity analyses.

DISCUSSION

In this study, we used a data-driven approach to identify multivariate FC patterns that underlie DD in a large sample of children, adolescents, and young adults. Our approach revealed that connectivity patterns of a region within the DMN—the dPFC—related to individual differences in DD. Further analyses revealed that higher DD was associated with increased FC of the dPFC with other regions within the DMN, and reduced FC with regions within the DAN and VAN. Taken together, these findings suggest that the dPFC may be a key node important for individual differences in impulsive choice within large-scale functional networks during resting-state imaging.

Notably, different parts of the dPFC are related to different aspects of DD, including the dlPFC, an executive control region, (Hare et al., 2014) and the dMPFC, implicated in processing future rewards and delay time (Wang et al., 2021). Other regions of the DMN, including the vmPFC and PCC, have been implicated in subjective valuation processes critical for decision-making (Pfeifer and Berkman, 2018; Bartra, McGuire, and Kable, 2013; Kable and Glimcher, 2007). Greater impulsivity has been associated with changes in how these regions represent reward features and value differences during DD tasks (Vanyukov et al., 2015; Koban et al., 2021). When interpreted

in the context of these previous findings, our results suggest that stronger integration between the dPFC and other hubs of the DMN involved in valuation could be associated with impulsive decision-making, consistent with at least one smaller study in younger adults (Jung et al., 2021).

We found that participants with a greater discount rate also showed greater anticorrelation between the dPFC and networks involved in attentional and cognitive control such as the DAN and VAN. This pattern mirrors resting-state functional segregation—or increased anticorrelation between disparate brain networks (Fair et al., 2007). Our results parallel previous studies showing that resting-state functional segregation between large-scale networks—for example, the connectivity of the DMN with the cingulo-opercular network, which is involved in cognitive control (Sadaghiani, and D'Esposito, 2014)—can predict DD (Chen, Guo, Suo, and Feng, 2018). This pattern of anticorrelation with the attention networks aligns with the frequently observed dissociation between task-positive attention networks and the task-negative DMN (Fox et al., 2005). These findings suggest that stronger connections between regions within the DMN, together with weaker connections between the DMN and attentional control networks, could underlie higher DD through changes in attentional control and reward valuation.

Prior work suggests that adolescence is an important period for the general organization of large-scale FC, in which changes in connectivity adhere to a sensorimotor-association gradient that culminates in the DMN, a network clearly implicated in our analyses (Sydnor et al., 2022; Margulies et al., 2016). Further, the FC of the dPFC is known to evolve throughout adolescence with a shift from general to more differentiated abilities (Li et al., 2022). There is also evidence for functional separation between regions of the dPFC including the dmPFC and dlPFC, both regions involved in DD (Li et al., 2022). Nonetheless, we found no associations between age and DD in our work.

Limitations

Several limitations of this work should be noted. First, our study is cross-sectional rather than longitudinal, which may have limited our ability to find associations between age and DD. However, the null effects seen in our sample do align with the inconsistent and small age effects in the DD literature as noted before (Romer, et al., 2017). Nonetheless, it is important to acknowledge that developmental changes in DD may occur at earlier ages than those studied here, and that longitudinal studies might detect developmental effects through measurement of within-person change documented in previous studies (Anandakumar et al., 2018; Achterberg et al., 2016). Second, the MDMR approach has limited sensitivity in many settings, potentially increasing the risk of type II error. For example, MDMR analysis is often insensitive to more focal changes because it summarizes differences in distributed multivariate patterns of connectivity (Misaki et al., 2018). Finally, our task used hypothetical rather than real rewards as part of the DD paradigm. However, previous research has not revealed differences between performance on DD tasks with real versus hypothetical rewards (Bickel et al., 2009).

Conclusions

We found that the pattern of dPFC connectivity is related to individual differences in impulsive choice during youth. Multivariate patterns associated with impulsive choice were driven primarily by increased connectivity between the dPFC and other parts of the DMN, as well as diminished connectivity with attention networks. Moving forward, the results from this data-driven analysis will be important to replicate. While speculative, these results also suggest that the dPFC may be a potential target for TMS and neuromodulatory therapies for conditions where impulsivity is prominent.

ACKNOWLEDGEMENTS:

This work was supported by the U.S. National Institute of Mental Health grants MH120174 (David R. Roalf), MH119185 (David R. Roalf), R01MH117014 (Ruben C. Gur, Raquel E. Gur), R01MH119219 (Ruben C. Gur, Raquel E. Gur), R01MH120482 (Theodore D. Satterthwaite), R01MH113550 (Theodore D. Satterthwaite), R01EB022573 (Theodore D. Satterthwaite), R37MH125829, (Theodore D. Satterthwaite), RC2MH089983 (Raquel E. Gur), RC2MH089924 (Raquel E. Gur), K99MH127293 (Bart Larsen), 2T32MH019112-29A1 (Erica Baller), R01MH113565 (Daniel H. Wolf), F31MH123063-01 (Adam Pines) and Deutsche Forschungsgemeinschaft (DFG, German Research Foundation) grant 269953372/GRK2150 (Martin Gell). There are no competing interests at this time.

DATA AVAILABILITY:

The Philadelphia Neurodevelopmental Cohort is a publicly available dataset at https://www.ncbi.nlm.nih.gov/projects/gap/cgi-bin/study.cgi?study_id=phs000607.v3.p2.

CODE AVAILABILITY:

All code and a reproducibility guide for this project is available at <https://github.com/PennLINC/pncite>.

REFERENCES

- Achterberg, M., Peper, J. S., Duijvenvoorde, A. C. K. van, Mandl, R. C. W., & Crone, E. A. (2016). Frontostriatal White Matter Integrity Predicts Development of Delay of Gratification: A Longitudinal Study. *Journal of Neuroscience*, 36(6), 1954–1961. <https://doi.org/10.1523/JNEUROSCI.3459-15.2016>
- Alexander-Bloch, A., Shou, H., Liu, S., Satterthwaite, T.D., Glahn, D.C., Shinohara, R.T., Vandekar, S.N., and Raznahan, A. (2018). On testing for spatial correspondence between maps of human brain structure and function. *Neuroimage* 178, 540–551. <https://doi.org/10.1016/j.neuroimage.2018.05.070>.
- Alves, P. N., Foulon, C., Karolis, V., Bzdok, D., Margulies, D. S., Volle, E., & Thiebaut de Schotten, M. (2019). An improved neuroanatomical model of the default-mode network reconciles previous neuroimaging and neuropathological findings. *Communications Biology*, 2(1), Article 1. <https://doi.org/10.1038/s42003-019-0611-3>
- Amlung, M., Marsden, E., Holshausen, K., Morris, V., Patel, H., Vedelago, L., Naish, K. R., Reed, D. D., & McCabe, R. E. (2019). Delay Discounting as a Transdiagnostic Process in Psychiatric Disorders: A Meta-analysis. *JAMA Psychiatry*, 76(11), 1176–1186. <https://doi.org/10.1001/jamapsychiatry.2019.2102>
- Anandakumar, J., Mills, K. L., Earl, E. A., Irwin, L., Miranda-Dominguez, O., Demeter, D. V., Walton-Weston, A., Karalunas, S., Nigg, J., & Fair, D. A. (2018). Individual differences in functional brain connectivity predict temporal discounting preference in the transition to adolescence. *Developmental Cognitive Neuroscience*, 34. <https://doi.org/10.1016/j.dcn.2018.07.003>
- Andrews-Hanna, J. R., Reidler, J. S., Sepulcre, J., Poulin, R., & Buckner, R. L. (2010). Functional-Anatomic Fractionation of the Brain's Default Network. *Neuron*, 65(4), 550–562. <https://doi.org/10.1016/j.neuron.2010.02.005>
- Avants, B. B., Tustison, N. J., Song, G., Cook, P. A., Klein, A., & Gee, J. C. (2011a). *A reproducible evaluation of ANTs similarity metric performance in brain image registration—PubMed*.
- Avants, B. B., Tustison, N. J., Wu, J., Cook, P. A., & Gee, J. C. (2011b). An open source multivariate framework for n-tissue segmentation with evaluation on public data. *Neuroinformatics*, 9(4). <https://doi.org/10.1007/s12021-011-9109-y>
- Avants, B., & Gee, J. C. (2004). Geodesic estimation for large deformation anatomical shape averaging and interpolation. *NeuroImage*, 23 Suppl 1. <https://doi.org/10.1016/j.neuroimage.2004.07.010>
- Avants, B.B., Epstein, C.L., Grossman, M. & Gee., J.C., (2008). *Symmetric diffeomorphic image registration with cross-correlation: Evaluating automated labeling of elderly and neurodegenerative brain*.
- Baller, E. B., Valcarcel, A. M., Adebimpe, A., Alexander-Bloch, A., Cui, Z., Gur, R. C., Gur, R. E., Larsen, B. L., Linn, K. A., O'Donnell, C. M., Pines, A. R., Raznahan, A., Roalf, D. R., Sydnor, V. J., Tapera, T. M., Tisdall, M. D., Vandekar, S., Xia, C. H., Detre, J. A., ... Satterthwaite, T. D. (2022). *Developmental coupling of cerebral blood flow and fMRI fluctuations in youth*.
- Bartra, O., McGuire, J. T., & Kable, J. W. (2013). The valuation system: A coordinate-based meta-analysis of BOLD fMRI experiments examining neural correlates of subjective value. *NeuroImage*, 76. <https://doi.org/10.1016/j.neuroimage.2013.02.063>

- Bickel, W. K., Jarmolowicz, D. P., Mueller, E. T., Koffarnus, M. N., & Gatchalian, K. M. (2012). Excessive Discounting of Delayed Reinforcers as a Trans-Disease Process Contributing to Addiction and Other Disease-Related Vulnerabilities: Emerging Evidence. *Pharmacology & Therapeutics*, 134(3), 287. <https://doi.org/10.1016/j.pharmthera.2012.02.004>
- Bickel, W. K., Pitcock, J. A., Yi, R., & Angtuaco, E. J. C. (2009). Congruence of BOLD Response across Intertemporal Choice Conditions: Fictive and Real Money Gains and Losses. *Journal of Neuroscience*, 29(27), 8839–8846. <https://doi.org/10.1523/JNEUROSCI.5319-08.2009>
- Buckner, R.L., and Krienen, F.M. (2013). The evolution of distributed association networks in the human brain. *Trends Cogn. Sci.* 17, 648–665. <https://doi.org/10.1016/j.tics.2013.09.017>
- Button, K., Ioannidis, J., Mokrysz, C. *et al.* Power failure: why small sample size undermines the reliability of neuroscience. *Nat Rev Neurosci* 14, 365–376 (2013). <https://doi.org/10.1038/nrn3475>
- Calluso, C., Tosoni, A., Pezzulo, G., Spadone, S., & Committeri, G. (2015). Interindividual Variability in Functional Connectivity as Long-Term Correlate of Temporal Discounting. *PLOS ONE*, 10(3), e0119710. <https://doi.org/10.1371/journal.pone.0119710>
- Chase, H. W., & Hogarth, L. (2011). Impulsivity and Symptoms of Nicotine Dependence in a Young Adult Population. *Nicotine & Tobacco Research*, 13(12), 1321–1325. <https://doi.org/10.1093/ntr/ntr114>
- Chen, Z., Guo, Y., & Feng, T. (2017). Delay discounting is predicted by scale-free dynamics of default mode network and salience network. *Neuroscience*, 362, 219–227. <https://doi.org/10.1016/j.neuroscience.2017.08.028>
- Chen, Z., Guo, Y., Suo, T., & Feng, T. (2018). Coupling and segregation of large-scale brain networks predict individual differences in delay discounting. *Biological Psychology*, 133. <https://doi.org/10.1016/j.biopsycho.2018.01.011>
- Ciric, R., Rosen, A. F. G., Erus, G., Cieslak, M., Adebimpe, A., Cook, P. A., Bassett, D. S., Davatzikos, C., Wolf, D. H., & Satterthwaite, T. D. (2018). Mitigating head motion artifact in functional connectivity MRI. *Nature Protocols*, 13(12). <https://doi.org/10.1038/s41596-018-0065-y>
- Ciric, R., Wolf, D. H., Power, J. D., Roalf, D. R., Baum, G. L., Ruparel, K., Shinohara, R. T., Elliott, M. A., Eickhoff, S. B., Davatzikos, C., Gur, R. C., Gur, R. E., Bassett, D. S., & Satterthwaite, T. S. (2017). Benchmarking of participant-level confound regression strategies for the control of motion artifact in studies of functional connectivity. *NeuroImage*. <https://doi.org/10.1016/j.neuroimage.2017.03.020>
- Costa Dias, T. G., Wilson, V. B., Bathula, D. R., Iyer, S. P., Mills, K. L., Thurlow, B. L., Stevens, C. A., Musser, E. D., Carpenter, S. D., Grayson, D. S., Mitchell, S. H., Nigg, J. T., & Fair, D. A. (2013). Reward circuit connectivity relates to delay discounting in children with attention-deficit/hyperactivity disorder. *European Neuropsychopharmacology: The Journal of the European College of Neuropsychopharmacology*, 23(1), 33–45. <https://doi.org/10.1016/j.euroneuro.2012.10.015>
- Dohmatob, E., Dumas, G., & Bzdok, D. (2020). Dark control: The default mode network as a reinforcement learning agent. *Human Brain Mapping*, 41(12), 3318. <https://doi.org/10.1002/hbm.25019>

- Eklund, A., Nichols, T. E., & Knutsson, H. (2016). Cluster failure: Why fMRI inferences for spatial extent have inflated false-positive rates. *PNAS*.
- Epstein, L. H., Salvy, S. J., Carr, K. A., Dearing, K. K., & Bickel, W. K. (2010). Food reinforcement, delay discounting and obesity. *Physiology & Behavior*, *100*(5), 438. <https://doi.org/10.1016/j.physbeh.2010.04.029>
- Fair, D. A., Dosenbach, N. U. F., Church, J. A., Cohen, A. L., Brahmbhatt, S., Miezin, F. M., Barch, D. M., Raichle, M. E., Petersen, S. E., & Schlaggar, B. L. (2007). Development of distinct control networks through segregation and integration. *Proceedings of the National Academy of Sciences*, *104*(33), 13507–13512. <https://doi.org/10.1073/pnas.0705843104>
- Fox, M. D., Snyder, A. Z., Vincent, J. L., Corbetta, M., Van Essen, D. C., & Raichle, M. E. (2005). The human brain is intrinsically organized into dynamic, anticorrelated functional networks. *Proceedings of the National Academy of Sciences*, *102*(27), 9673–9678. <https://doi.org/10.1073/pnas.0504136102>
- Greve, D. N., & Fischl, B. (2009). Accurate and robust brain image alignment using boundary-based registration. *NeuroImage*, *48*(1). <https://doi.org/10.1016/j.neuroimage.2009.06.060>
- Gur, R. C., Richard, J., Calkins, M. E., Chiavacci, R., Hansen, J. A., Bilker, W. B., Loughhead, J., Connolly, J. J., Qiu, H., Mentch, F. D., Abou-Sleiman, P. M., Hakonarson, H., & Gur, R. E. (2012). Age group and sex differences in performance on a computerized neurocognitive battery in children age 8-21. *Neuropsychology*, *26*(2), 251–265. <https://doi.org/10.1037/a0026712>
- Gur, R. C., Richard, J., Hughett, P., Calkins, M. E., Macy, L., Bilker, W. B., Brensinger, C., & Gur, R. E. (2010). A cognitive neuroscience-based computerized battery for efficient measurement of individual differences: Standardization and initial construct validation. *Journal of Neuroscience Methods*, *187*(2), 254–262. <https://doi.org/10.1016/j.jneumeth.2009.11.017>
- Hallquist, M. N., Hwang, K., & Luna, B. (2013). The nuisance of nuisance regression: Spectral misspecification in a common approach to resting-state fMRI preprocessing reintroduces noise and obscures functional connectivity. *NeuroImage*, *82*. <https://doi.org/10.1016/j.neuroimage.2013.05.116>
- Hare, T. A., Hakimi, S., & Rangel, A. (2014). Activity in dlPFC and its effective connectivity to vmPFC are associated with temporal discounting. *Frontiers in Neuroscience*, *0*. <https://doi.org/10.3389/fnins.2014.00050>
- Hirsh, J. B., Morisano, D., & Peterson, J. B. (2008). Delay discounting: Interactions between personality and cognitive ability. *Journal of Research in Personality*, *42*(6), 1646–1650. <https://doi.org/10.1016/j.jrp.2008.07.005>
- Jenkinson, M. (2003). Fast, automated, N-dimensional phase-unwrapping algorithm. *Magnetic Resonance in Medicine*, *49*(1). <https://doi.org/10.1002/mrm.10354>
- Jenkinson, M., Bannister, P., Brady, M., & Smith, S. (2002). Improved optimization for the robust and accurate linear registration and motion correction of brain images. *NeuroImage*, *17*(2). [https://doi.org/10.1016/s1053-8119\(02\)91132-8](https://doi.org/10.1016/s1053-8119(02)91132-8)
- Jung, W. H. (2021). Individual Differences of Functional Brain Networks from Resting-state fMRI and Delay Discount Rate. *Korean Journal of Cognitive and Biological Psychology*, *33*(1), 15–29. <https://doi.org/10.22172/cogbio.2021.33.1.002>

- Kable, J. W., & Glimcher, P. W. (2007). The neural correlates of subjective value during intertemporal choice. *Nature Neuroscience*, *10*(12). <https://doi.org/10.1038/nn2007>
- Kable, J. W., & Glimcher, P. W. (2010). An “as soon as possible” effect in human intertemporal decision making: Behavioral evidence and neural mechanisms. *Journal of Neurophysiology*, *103*(5). <https://doi.org/10.1152/jn.00177.2009>
- Kable, J. W., & Levy, I. (2015). Neural markers of individual differences in decision-making. *Current Opinion in Behavioral Sciences*, *5*, 100. <https://doi.org/10.1016/j.cobeha.2015.08.004>
- Kirby, K. N. (2009). One-year temporal stability of delay-discount rates. *Psychonomic Bulletin & Review*, *16*(3), 457–462. <https://doi.org/10.3758/PBR.16.3.457>
- Klein, A., Andersson, J., Ardekani, B. A., Ashburner, J., Avants, B., Chiang, M. C., Christensen, G. E., Collins, D. I., Gee, J., Hellier, P., Song, J. H., Jenkinson, M., Lepage, C., Rueckert, D., Thompson, P., Vercauteren, T., Woods, R. P., Mann, J. J., & R.V., P. (2009). Evaluation of 14 nonlinear deformation algorithms applied to human brain MRI registration. *NeuroImage*, *46*(3). <https://doi.org/10.1016/j.neuroimage.2008.12.037>
- Koban, L., Lee, S., Schelski, D. S., Simon, M.-C., Lerman, C., Weber, B., Kable, J. W., & Plassmann, H. (2021). An fMRI-based brain marker predicts individual differences in delay discounting. *BioRxiv*. <https://doi.org/10.1101/2021.03.18.435969>
- Lempert, K. M., Steinglass, J. E., Pinto, A., Kable, J. W., & Simpson, H. B. (2019). Can delay discounting deliver on the promise of RDoC? *Psychological Medicine*, *49*(2), 190–199. <https://doi.org/10.1017/S0033291718001770>
- Li, N., Ma, N., Liu, Y., He, X.-S., Sun, D.-L., Fu, X.-M., Zhang, X., Han, S., & Zhang, D.-R. (2013). Resting-State Functional Connectivity Predicts Impulsivity in Economic Decision-Making. *Journal of Neuroscience*, *33*(11), 4886–4895. <https://doi.org/10.1523/JNEUROSCI.1342-12.2013>
- Li, W., Shi, W., Wang, H., Li, J., Cui, Y., Li, K., Cheng, L., Lu, Y., Ma, L., Chu, C., Song, M., Yang, Z., Banaschewski, T., Bokde, A. L. W., Desrivieres, S., Flor, H., Grigis, A., Garavan, H., Gowland, P., ... Consortium, I. (2022). *Anatomical connectivity profile development constrains medial-lateral topography in the dorsal prefrontal cortex* (p. 2022.02.07.479322). bioRxiv. <https://doi.org/10.1101/2022.02.07.479322>
- Madden, G. J., Begotka, A. M., Raiff, B. R., & Kastern, L. L. (2003). Delay discounting of real and hypothetical rewards. *Experimental and Clinical Psychopharmacology*, *11*(2), 139–145. <https://doi.org/10.1037/1064-1297.11.2.139>
- Mahalingam, V., Palkovics, M., Kosinski, M., Cek, I., & Stillwell, D. (2016). A Computer Adaptive Measure of Delay Discounting. *Assessment*. <https://doi.org/10.1177/1073191116680448>
- Marek, S., Tervo-Clemmens, B., Calabro, F. J., Montez, D. F., Kay, B. P., Hatoum, A. S., Donohue, M. R., Foran, W., Miller, R. L., Hendrickson, T. J., Malone, S. M., Kandala, S., Feczko, E., Miranda-Dominguez, O., Graham, A. M., Earl, E. A., Perrone, A. J., Cordova, M., Doyle, O., ... Dosenbach, N. U. F. (2022). Reproducible brain-wide association studies require thousands of individuals. *Nature*, *603*(7902), Article 7902. <https://doi.org/10.1038/s41586-022-04492-9>
- Margulies, D. S., Ghosh, S. S., Goulas, A., Falkiewicz, M., Huntenburg, J. M., Langs, G., Bezgin, G., Eickhoff, S. B., Castellanos, F. X., Petrides, M., Jefferies, E., & Smallwood, J. (2016). Situating the default-mode network along a principal gradient of macroscale

- cortical organization. *Proceedings of the National Academy of Sciences*, 113(44), 12574–12579. <https://doi.org/10.1073/pnas.1608282113>
- Mazur JE. (1987) An adjusting procedure for studying delayed reinforcement. *Quantitative analyses of behavior, Vol. 5: the effect of delay and of intervening events on reinforcement value* (Commons ML, Mazur JE, Nevin JA, eds) pp 55–73. Hillsdale, NJ: Lawrence Erlbaum.
- Misaki, M., Phillips, R., Zotev, V., Wong, C.-K., Wurfel, B. E., Krueger, F., Feldner, M., & Bodurka, J. (2018). Real-time fMRI amygdala neurofeedback positive emotional training normalized resting-state functional connectivity in combat veterans with and without PTSD: A connectome-wide investigation. *NeuroImage: Clinical*, 20, 543. <https://doi.org/10.1016/j.nicl.2018.08.025>
- Mischel, W., Shoda, Y., & Rodriguez, M. L. (1989). Delay of Gratification in Children. *Science*, 244(4907), 933–938. <https://doi.org/10.1126/science.2658056>
- Ortiz, N., Parsons, A., Whelan, R., Brennan, K., Agan, M. L. F., O’Connell, R., Bramham, J., & laht, H. (2015). Decreased frontal, striatal and cerebellar activation in adults with ADHD during an adaptive delay discounting task. *Acta Neurobiologiae Experimentalis*, 75(3), 326–338.
- Pehlivanova, M., Wolf, D. H., Sotiras, A., Kaczkurkin, A. N., Moore, T. M., Ciric, R., Cook, P. A., Garza, A. G. de L., Rosen, A. F. G., Ruparel, K., Sharma, A., Shinohara, R. T., Roalf, D. R., Gur, R. C., Davatzikos, C., Gur, R. E., Kable, J. W., & Satterthwaite, T. D. (2018). Diminished Cortical Thickness Is Associated with Impulsive Choice in Adolescence. *The Journal of Neuroscience*, 38(10), 2471. <https://doi.org/10.1523/JNEUROSCI.2200-17.2018>
- Peters J. & Büchel C. (2010). Episodic future thinking reduces reward delay discounting through an enhancement of prefrontal-mediotemporal interactions. *Neuron*, 66(1). <https://doi.org/10.1016/j.neuron.2010.03.026>
- Pfeifer, J. H., & Berkman, E. T. (2018). The Development of Self and Identity in Adolescence: Neural Evidence and Implications for a Value-Based Choice Perspective on Motivated Behavior. *Child Development Perspectives*, 12(3). <https://doi.org/10.1111/cdep.12279>
- Raut, R.V., Snyder, A.Z., and Raichle, M.E. (2020). Hierarchical dynamics as a macroscopic organizing principle of the human brain. *PNAS* 117, 2089020897. <https://doi.org/10.1073/pnas.2003383117>.
- Romer, D., Reyna, V. F., & Satterthwaite, T. D. (2017). Beyond stereotypes of adolescent risk taking: Placing the adolescent brain in developmental context. *Developmental Cognitive Neuroscience*, 27, 19–34. <https://doi.org/10.1016/j.dcn.2017.07.007>
- Rosch, K. S., Mostofsky, S. H., & Nebel, M. B. (2018). ADHD-related sex differences in fronto-subcortical intrinsic functional connectivity and associations with delay discounting. *Journal of Neurodevelopmental Disorders*, 10(1), 34. <https://doi.org/10.1186/s11689-018-9254-9>
- Rosen, A. F. G., Roalf, D. R., Ruparel, K., Blake, J., Seelaus, K., Villa, L. P., Ciric, R., Cook, P. A., Davatzikos, C., Elliott, M. A., Garcia de La Garza, A., Gennatas, E. D., Quarmley, M., Schmitt, J. E., Shinohara, R. T., Tisdall, M. D., Craddock, R. C., Gur, R. E., Gur, R. C., & Satterthwaite, T. D. (2018). Quantitative assessment of structural image quality. *NeuroImage*, 169, 407–418. <https://doi.org/10.1016/j.neuroimage.2017.12.059>

- Sadaghiani, S., & D'Esposito, M. (2015). Functional Characterization of the Cingulo-Opercular Network in the Maintenance of Tonic Alertness. *Cerebral Cortex*, 25(9), 2763–2773. <https://doi.org/10.1093/cercor/bhu072>
- Satterthwaite, T. D., Elliott, M. A., Gerraty, R. T., Ruparel, K., Loughhead, J., Calkins, M. E., Eickhoff, S. B., Hakonarson, H., Gur, R. C., Gur, R. E., & Wolf, D. H. (2013). An Improved Framework for Confound Regression and Filtering for Control of Motion Artifact in the Preprocessing of Resting-State Functional Connectivity Data. *NeuroImage*, 64. <https://doi.org/10.1016/j.neuroimage.2012.08.052>
- Satterthwaite, T. D., Elliott, M. A., Ruparel, K., Loughhead, J., Prabhakaran, K., Calkins, M. E., Hopson, R., Jackson, C., Keefe, J., Riley, M., Mensh, F. D., Sleiman, P., Verma, R., Davatzikos, C., Hakonarson, H., Gur, R. C., & Gur, R. E. (2014). Neuroimaging of the Philadelphia Neurodevelopmental Cohort. *NeuroImage*, 86, 544. <https://doi.org/10.1016/j.neuroimage.2013.07.064>
- Satterthwaite, T. D., Vandekar, S. N., Wolf, D. H., Bassett, D. S., Ruparel, K., Shehzad, Z., Craddock, R. C., Shinohara, R. T., Moore, T. M., Gennatas, E. D., Jackson, C., Roalf, D. R., Milham, M. P., Calkins, M. E., Hakonarson, H., Gur, R. C., & Gur, R. E. (2015). Connectome-wide network analysis of youth with Psychosis-Spectrum symptoms. *Molecular Psychiatry*, 20(12). <https://doi.org/10.1038/mp.2015.66>
- Satterthwaite T.D., Connolly J.J., Ruparel K., Calkins M.E., Jackson C., Elliott Ma, Roalf D.R., Hopson R., Prabhakaran K., Behr M., Qiu H., Mentch F.D., Chiavacci R., Sleiman P.M.A., Gur R.C., Hakonarson H., & Gur R.E. (2016). The Philadelphia Neurodevelopmental Cohort: A publicly available resource for the study of normal and abnormal brain development in youth. *NeuroImage*, 124(Pt B). <https://doi.org/10.1016/j.neuroimage.2015.03.056>
- Schüller, C. B., Kuhn, J., Jessen, F., & Hu, X. (2019). Neuronal correlates of delay discounting in healthy subjects and its implication for addiction: An ALE meta-analysis study. *The American Journal of Drug and Alcohol Abuse*. <https://www.tandfonline.com/doi/abs/10.1080/00952990.2018.1557675>
- Senecal, N., Wang, T., Thompson, E., & Kable, J. W. (2012). Normative arguments from experts and peers reduce delay discounting. *Judgment and Decision Making*, 7(5), 568. <https://www.ncbi.nlm.nih.gov/pmc/articles/PMC3626281/>
- Sharma, A., Wolf, D. H., Ciric, R., Kable, J. W., Moore, T. M., Vandekar, S. N., Katchmar, N., Daldal, A., Ruparel, K., Davatzikos, C., Elliott, M. A., Calkins, M. E., Shinohara, R. T., Bassett, D. S., & Satterthwaite, T. D. (2017). Connectome-Wide Analysis Reveals Common Dimensional Reward Deficits Across Mood and Psychotic Disorders. *The American Journal of Psychiatry*, 174(7), 657. <https://doi.org/10.1176/appi.ajp.2016.16070774>
- Shehzad, Z., Kelly, C., Reiss, P. T., Cameron Craddock, R., Emerson, J. W., McMahon, K., Copland, D. A., Castellanos, F. X., & Milham, M. P. (2014). A multivariate distance-based analytic framework for connectome-wide association studies. *NeuroImage*, 93 Pt 1(0 1). <https://doi.org/10.1016/j.neuroimage.2014.02.024>
- Souther, M. K., Boateng, B., & Kable, J. W. (2022). A meta-analysis of neural systems underlying delay discounting: Implications for transdiagnostic research. *BioRxiv*, 2022.10.12.511959. <https://doi.org/10.1101/2022.10.12.511959>
- Sydnor, V. J., Larsen, B., Seidlitz, J., Adebimpe, A., Alexander-Bloch, A., Bassett, D. S., Bertolero, M. A., Cieslak, M., Covitz, S., Fan, Y., Gur, R. E., Gur, R. C., Mackey, A. P.,

- Moore, T. M., Roalf, D. R., Shinohara, R. T., & Satterthwaite, T. D. (2022). Intrinsic Activity Develops Along a Sensorimotor-Association Cortical Axis in Youth. *BioRxiv*, 2022.08.15.503994. <https://doi.org/10.1101/2022.08.15.503994>
- Thomas Yeo, B.T., Krienen, F.M., Sepulcre, J., Sabuncu, M.R., Lashkari, D., Hollinshead, M., Roffman, J.L., Smoller, J.W., Zöllei, L., Polimeni, J.R., et al. (2011). The organization of the human cerebral cortex estimated by intrinsic functional connectivity. *J. Neurophysiol.* 106, 1125–1165. <https://doi.org/10.1152/jn.00338.2011>
- Tjur T. (2009) Coefficients of determination in logistic regression models—a new proposal: the coefficient of discrimination. *Am Stat* 63:366–372. <https://doi.org/10.1198/tast.2009.08210>
- Tustison, N. J., Avants, B. B., Cook, P. A., Zheng, Y., Egan, A., Yushkevich, P. A., & Gee, J. C. (2010). N4ITK: Improved N3 bias correction. *IEEE Transactions on Medical Imaging*, 29(6). <https://doi.org/10.1109/TMI.2010.2046908>
- Tustison, N. J., Pa, C., Klein, A., Song, G., Das, S. R., Duda, J. T., Kandel, B. M., Strien, N. van, Stone, J. R., Gee, J. C., & Avants, B. B. (2014). Large-scale evaluation of ANTs and FreeSurfer cortical thickness measurements. *NeuroImage*, 99. <https://doi.org/10.1016/j.neuroimage.2014.05.044>
- Uddin, L. Q., Kelly, A. M. C., Biswal, B. B., Castellanos, F. X., & Milham, M. P. (2009). Functional connectivity of default mode network components: Correlation, anticorrelation, and causality. *Human Brain Mapping*, 30(2), 625–637. <https://doi.org/10.1002/hbm.20531>
- Vanyukov, P. M., Szanto, K., Hallquist, M. N., Siegle, G. J., Charles F. Reynolds, I. I. I., Forman, S. D., Aizenstein, H. J., & Dombrovski, A. Y. (2016). Paralimbic and lateral prefrontal encoding of reward value during intertemporal choice in attempted suicide.
- Wang, S., Zhou, M., Chen, T., Yang, X., Chen, G., & Gong, Q. (2017). Delay discounting is associated with the fractional amplitude of low-frequency fluctuations and resting-state functional connectivity in late adolescence. *Scientific Reports*, 7(1), Article 1. <https://doi.org/10.1038/s41598-017-11109-z>
- Psychological Medicine*, 46(2), 381. <https://doi.org/10.1017/S0033291715001890>
- Wang, Q., Wang, Y., Wang, P., Peng, M., Zhang, M., Zhu, Y., Wei, S., Chen, C., Chen, X., Luo, S., & Bai, X. (2021). Neural representations of the amount and the delay time of reward in intertemporal decision making. *Human Brain Mapping*, 42(11), 3450–3469. <https://doi.org/10.1002/hbm.25445>
- Weller, R. E., Avsar, K. B., Cox, J. E., Reid, M. A., White, D. M., & Lahti, A. C. (2014). Delay discounting and task performance consistency in patients with schizophrenia. *Psychiatry Research*, 215(2), 286–293. <https://doi.org/10.1016/j.psychres.2013.11.013>
- Woolrich, M. W., Behrens, T. E., Beckmann, C. F., Jenkinson, M., & Smith, S. M. (2004). Multilevel linear modelling for fMRI group analysis using Bayesian inference. *NeuroImage*, 21(4). <https://doi.org/10.1016/j.neuroimage.2003.12.023>